



HAL
open science

Design of Oil Insulated SiC Diode Rectifier for an MVDC SST

Pierre Le Métayer, Hugo Reynes, Piotr Dworakowski, Cyril Buttay, Drazen Dujic

► **To cite this version:**

Pierre Le Métayer, Hugo Reynes, Piotr Dworakowski, Cyril Buttay, Drazen Dujic. Design of Oil Insulated SiC Diode Rectifier for an MVDC SST. International Exhibition and Conference for Power Electronics, Intelligent Motion, Renewable Energy and Energy Management (PCIM Europe 2023), May 2023, Nuremberg, Germany. pp.566091039, 10.30420/566091039 . hal-04153731

HAL Id: hal-04153731

<https://hal.science/hal-04153731v1>

Submitted on 6 Jul 2023

HAL is a multi-disciplinary open access archive for the deposit and dissemination of scientific research documents, whether they are published or not. The documents may come from teaching and research institutions in France or abroad, or from public or private research centers.

L'archive ouverte pluridisciplinaire **HAL**, est destinée au dépôt et à la diffusion de documents scientifiques de niveau recherche, publiés ou non, émanant des établissements d'enseignement et de recherche français ou étrangers, des laboratoires publics ou privés.

Design of Oil Insulated SiC Diode Rectifier for an MVDC SST

Pierre Le Metayer^{1,2}, Hugo Reynes¹, Piotr Dworakowski¹, Cyril Buttay², Drazen Dujic³

¹ SuperGrid Institute, 69100 Villeurbanne, France

² Univ Lyon, CNRS, INSA Lyon, Université Claude Bernard Lyon 1, Ecole Centrale de Lyon, Ampère, UMR 5005, 69621 Villeurbanne, France

³ Ecole Polytechnique Fédérale de Lausanne (EPFL), Power Electronics Laboratory, Switzerland

Corresponding author: Pierre Le Metayer, pierre.lemetayer@supergrid-institute.com

Abstract

A DC solid-state transformer is needed to interconnect PV sources to a medium voltage DC network. Due to the application requirements, unidirectional high step-up conversion is proposed. Immersion of the complete medium-voltage-side of the converter in transformer oil is proposed to achieve compact design. In this paper, we present the integration of the medium voltage and medium frequency diode rectifier in terms of cooling, dielectric design, and chemical compatibility, relying on printed circuit board technology.

1 Introduction

Medium voltage direct current (MVDC) collection networks for photovoltaic (PV) installations have been discussed in the literature as a way to lower power losses [1]. A DC-DC converter, or DC solid-state transformer (DC-SST), is required to interface the low voltage PV arrays (typically 1.5 kV) to the MVDC network. Equivalences can be drawn between state-of-the-art MVAC installations and the MVDC ones, as shown in Fig. 1. The maximum power point tracking (MPPT) function is realized in both cases by DC-DC converters. The string inverters of the MVAC solution can be seen in the MVDC case as merged together into a single centralized inverter which ensures connection to the existing AC grid. The voltage step-up function of the 50 Hz AC string transformer is performed by the DC-SST.

Considering string inverters as references [2], the DC-SST power is set to 250 kW. A symmetric monopole MVDC collection network voltage of ± 10 kV is considered according to [3]. As the power is only flowing from the PV sources to the MVDC network, a unidirectional converter topology is selected.

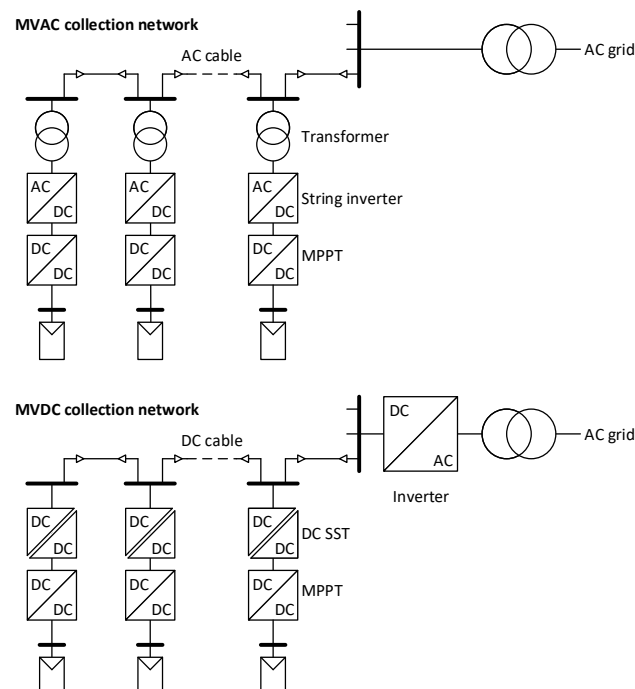


Fig. 1: PV MVAC versus MVDC power collection network diagram.

For the shift from MVAC to MVDC collection network to make sense, the DC-SST must be of at least the same efficiency and size as an equivalent 50 Hz transformer, despite its higher complexity (component count, control, etc.). Compactness is a particular concern: although the Medium-Frequency Transformer (MFT) used in the DC-DC converter is much smaller than a 50 Hz transformer with the same power ratings, the large insulation distances required in air between all the components of the MV side may result in a bulky converter.

Therefore, we propose to use a dielectric fluid, particularly the synthetic ester MIDEAL 7131 [4] (referred to as “oil”) as an insulating material and cooling solution, not only for the MFT, but also for the complete MV circuit of the DC-SST, so that insulation distances can be minimized. An illustration of the complete DC-SST mechanical design is shown in Fig. 2 with its schematic in Fig. 3. The oil tank integrates the MFT, rectifier and output filter composed of inductors and capacitors.

Because of the low converter output current (12.5 A), the rectifier is implemented using discrete diodes in standard through-hole TO-247 package mounted on a printed circuit board (PCB). 1.7 kV SiC diodes were found to be readily available and to offer low conduction losses. The electrical design of a medium voltage rectifier based on a series connection of low voltage SiC diodes has already been discussed in [5], [6], but little details were given in terms of integration.

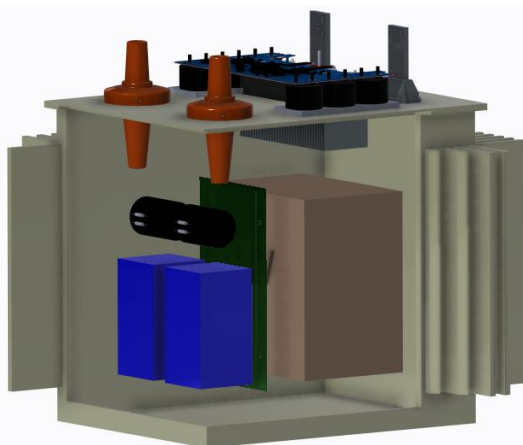


Fig. 2: DC-SST mechanical arrangement with MFT (brown), rectifier (green), inductors (blue) and capacitors (black) immersed in the oil tank and low voltage inverter sitting on top of the tank.

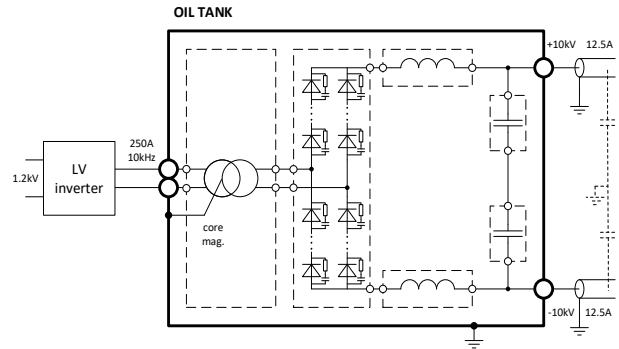


Fig. 3: Schematic of the converter, with entire MV circuit inside of the tank and LV inverter outside of the tank.

The use of oil-immersion cooling for PCB components has mostly been studied in the context of data centers low power servers [7], with a focus on improvements of thermal performance. Dielectric breakdown of liquid-insulated PCB was studied in [8] but is limited to 35 μm -thick copper traces, whereas thicker copper would be needed for the current levels involved in DC-SST applications. The impact of immersion of electronic components into the oil has mostly been studied regarding thermo-mechanical properties [9]. The chemical compatibility of the oil with the components must be verified in order to prevent degradation and damage of any of the involved elements.

This paper discusses the challenges of the design of a medium voltage PCB-implemented diode rectifier as part of an oil-immersed DC-SST. The cooling, dielectric design, and chemical compatibility topics are specifically addressed in the context of DC-SST and recommendations are given.

2 Oil cooling for the PCB-based rectifier

As presented in [6], the diodes selected for such a low current rectifier are packaged in standard TO-247 packages. The exchange surface with surrounding oil of this small package is limited and it is thus common to attach it to a finned heatsink, altering the favorable thin and flat form factor of the PCB. Indeed, in our case, using heatsinks attached to the diode packages is not desirable as it increases the box volume of the rectifier and therefore the total volume of the tank. Also, although oil has a better heat carrying capability than air, a DC-SST such as presented in Fig. 2 would rely on natural convection (whereas air cooling can be improved using forced convection), resulting in lim-

ited heat exchange coefficients. Therefore, effective use of oil to cool the diodes requires increasing the heat exchange surface around the diodes by creating patterned copper patches to form thermal vias on both sides of the board. These “flat heatsinks” can be seen in Fig. 4.

2.1 Design of oil cooled PCB rectifier

A 4 kV full bridge rectifier is realized following the electrical design presented in [6] with four 1.7 kV diodes connected in series per diode function. The concept presented above is used for the thermal design.

In order to choose the size of the copper patch around each diode, a simplified thermal model is used. It is considered that all of the copper surfaces on each side of the board represent a complete plate of surface S and height H . The model of the Vertical Parallel Plates [10] is used, with the second plate representing the MFT as shown in Fig. 2, and with the space between the two plates defined as L . This enables to compute the thermal resistance $R_{th_conv_oil}$ of the rectifier to oil interface with the equations below and the MIDEL 7131 properties given in Table 1.

$$Gr = \frac{g \beta \Delta T L^3}{\nu^2} \quad (1)$$

$$Pr = \frac{c_p \nu \rho}{\lambda} \quad (2)$$

$$Ra = Gr Pr \quad (3)$$

$$\widetilde{Ra} = Ra \frac{L}{H} \quad (4)$$

$$Nu = \left(\frac{576}{\widetilde{Ra}^2} + \frac{2.873}{\widetilde{Ra}^{0.5}} \right)^{-0.5} \quad (5)$$

$$R_{th_conv_oil} = \frac{L}{Nu \lambda S} \quad (6)$$

With the values used in this study given in Table 1, it is found that the space between the two plates has little to no influence on the thermal resistance.

The surface of a copper patch is designed so the junction temperature of the diode does not exceed 100°C, considering losses corresponding to the

operation at nominal current, with the oil temperature being 60°C. One should note that this is quite conservative, as SiC diodes can operate with junction temperatures above 150°C. The junction-to-case thermal resistance of the diode R_{th_jc} and the case-to-patch thermal resistance R_{th_cp} are known (Table 1) and patch dimensions are adjusted in order to obtain the required $R_{th_conv_oil}$. This results in the design shown in Fig. 4, with identical copper patches on both sides of the PCB. The complete PCB size is 19 cm by 27 cm. The individual surface of a copper patch is $S_{patch_face} = 13.5 \text{ cm}^2$, resulting in the total exchange surface $S = 432 \text{ cm}^2$.

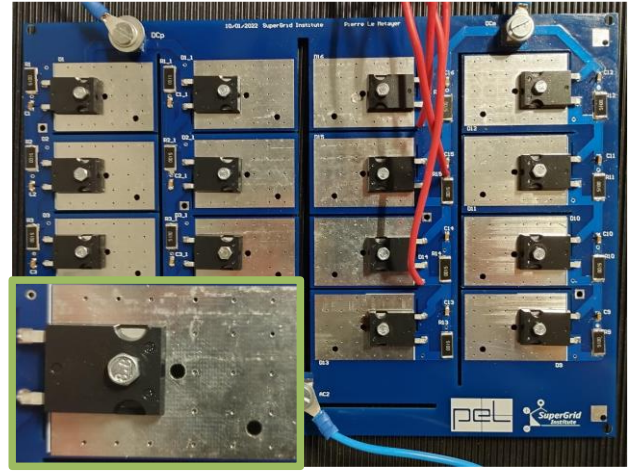


Fig. 4: 4 kV PCB-implemented diode rectifier, with zoom on patterned copper patch used as heatsinks on both sides (bigger holes are for thermocouple mounting).

Tab. 1: Model parameters.

| PCB parameters | |
|--|---------------------------------------|
| Height of the PCB H | 19 cm |
| Exchange surface S | 432 cm ² |
| Gap between 2 “plates” L | > 5 mm |
| Midel 7131 properties at 60°C | |
| Thermal expansion coefficient β | 77e ⁻⁵ /°C |
| Kinematic viscosity ν | 13.7e ⁻⁶ m ² /s |
| Specific heat capacity c_p | 1995 J/kg °C |
| Density ρ | 939 kg/m ³ |
| Thermal conductivity λ | 0.144 W/m °C |
| Diode parameters | |
| Diode model | Genesic GD25MPS17H |
| Junction to case thermal resistance R_{th_jc} | 0.3567 °C/W |
| Case to patch thermal resistance R_{th_cp} | 0.2151 °C/W |

2.2 Experimental results

The rectifier shown in Fig. 4 is tested at nominal power losses to validate the performance of the presented thermal design. The test set-up including the oil reservoir, pre-heating system, and rectifier board can be seen in Fig. 5 and Fig. 6.

The case temperatures of 4 vertically stacked diodes are measured with thermocouples. The MIDEL 7131 oil in which the rectifier is immersed is first heated up to 60°C by resistors in front of the PCB, to represent the DC-SST oil tank environment. The diode current corresponding to the nominal losses of 116 W is reached by applying the correct biasing voltage with a DC source. Results can be seen in Fig. 7.

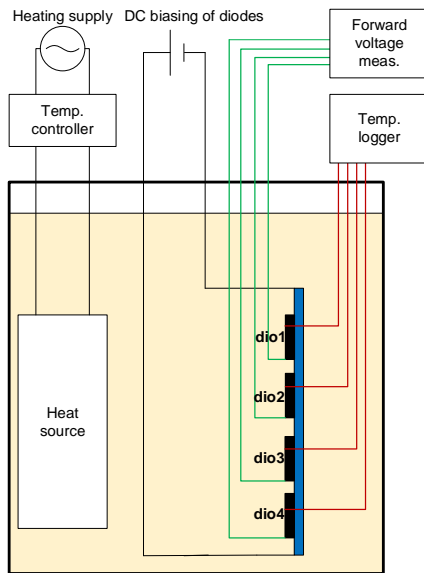


Fig. 5: Schematic of the test set-up of oil-immersed diode rectifier PCB represented in blue.

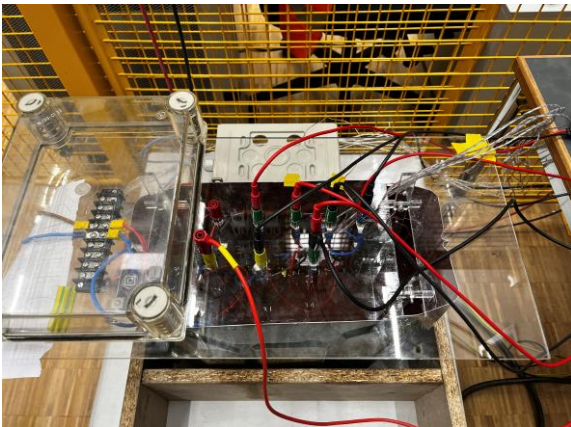


Fig. 6: Test set-up of the 4 kV prototype of oil-immersed diode rectifier PCB.

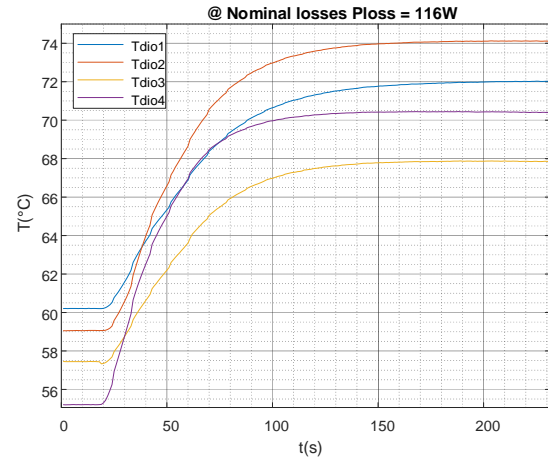


Fig. 7: Temperature of diodes for a power loss step from zero to nominal diode power loss.

One can first observe that the initial temperature is not 60°C for all diodes. Indeed the pre-heating was done measuring the oil temperature near the top of the reservoir. Thus the initial temperatures of some diodes is lower than 60°C, with the diodes in the bottom of the reservoir having lower temperatures. The maximum final case temperature is 74°C. Based on the value of $R_{th_{jc}}$ and the previously estimated case-to-patch thermal resistance $R_{th_{cp}}$ results in the junction temperature of 90.6°C. This is well below the limit originally fixed. This gives the conclusion that the model used is sufficient to design a thermally safe rectifier but a better model should be developed if the size of the copper patches needs to be optimized. Less conservative design margins on the junction temperature of the diode could also be taken to reduce the copper patch size.

It can be observed in Fig. 7 that temperature increases are different from diode to diode as the final temperatures are not correlated similarly as in the initial state. This can be mainly explained by differences in forward voltages and thus power losses as can be seen in Table 2.

Tab. 2: Forward voltages and temperature increases of series connected diodes at nominal losses

| Diode | Forward voltage | ΔT |
|-------|-----------------|------------|
| Dio1 | 1.11 V | 12.7°C |
| Dio2 | 1.18 V | 15.2°C |
| Dio3 | 1.09 V | 10.4°C |
| Dio4 | 1.16 V | 15.1°C |

3 Dielectric design of PCB-based rectifier

When designing the rectifier for higher rated voltages, the objective of keeping a small volume will lead to layouts where some traces with high voltage differences run close to each other. Thus, to keep a safe but compact design, the necessary insulation distances must be precisely known. The breakdown voltage of the gap between two traces on sample PCBs immersed in MIDELO 7131 oil is thus experimentally tested. The influence of the oil quality is also studied. Indeed, the dielectric strength of the oil is usually given for oil especially treated to remove impurity particles and humidity. The oil quality can degrade during operation, especially in the case of a free-breathing tank.

3.1 Test set-up

The same set-up is used for breakdown voltage and partial discharge measurements. The voltage is applied on the sample PCBs using an auto transformer connected to a 100 kV step up transformer. A 1.04 μF coupling capacitor is used for electrical PD measurements in compliance with the IEC 60270 standard. An Omicron MPD600 system is used to detect and record the PD activity. The partial discharge inception voltage (PDIV) is taken as the voltage value after which a sustained PD activity is observed over the 10 pC threshold. The voltage is continuously raised at approximately 1 kV/s until breakdown occurs. The last voltage value is taken as the breakdown voltage. Voltage levels are given as RMS values.

A PCB with two electrodes made of 70 μm thick copper traces and a 3 mm gap is used as test sample as shown in Fig. 8. One electrode is connected to the output of the high-voltage transformer and the other to the ground. Tests are performed in a box with plastic separators so the oil doesn't flow to the next sample after a breakdown (Fig. 9). Tests are performed with treated and non-treated oil. Each test configuration is performed with 10 samples.



Fig. 8: Sample PCB with 3 mm gap and 70 μm thick traces



Fig. 9: Test set-up of the PCB samples, after a batch of tests (black spots where breakdown happened)

3.2 Experimental results

The results are presented using Weibull plots. The sample results are fitted to a two-parameter cumulative Weibull distribution function:

$$F(V) = 1 - \exp\left[-\left(\frac{V}{\alpha}\right)^\beta\right] \quad (6)$$

with V the breakdown voltage or PDIV, α the scale factor and β the shape parameter.

Results for breakdown voltage are shown in Fig. 10 and for PDIV in Fig. 11. It can be seen that most of the data points are linear meaning a good fit with the Weibull function. The Weibull parameters are summarized in Table 3.

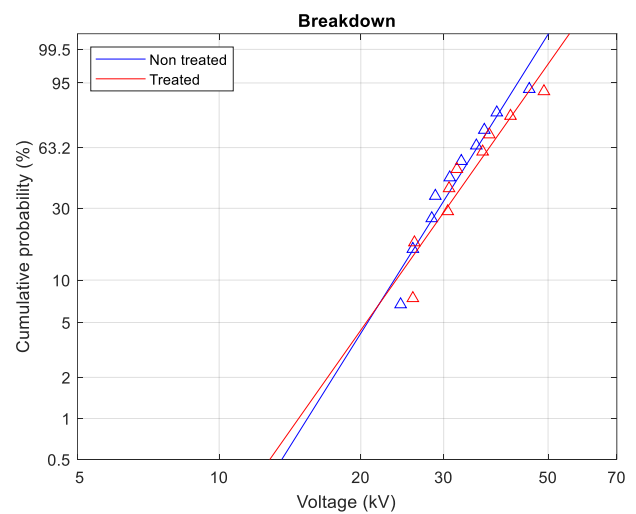


Fig. 10: Weibull plots for breakdown voltage in treated and non-treated oil. Samples represented by triangles and Weibull distribution in full line

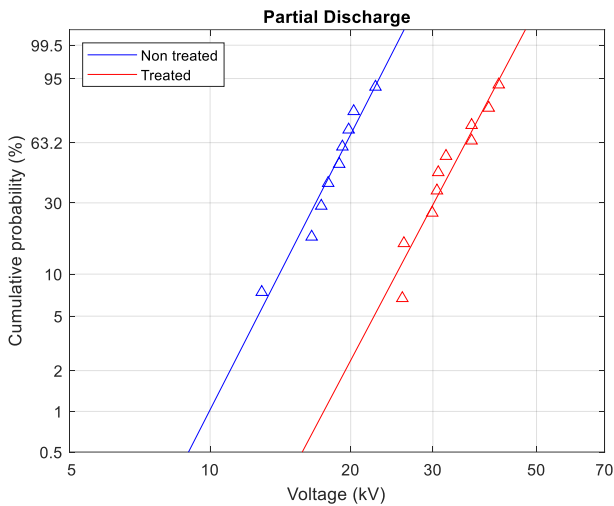


Fig. 11: Weibull plots for PDIV in treated and non-treated oil. Samples represented by triangles and Weibull distribution in full line

Tab. 3: Weibull parameters for breakdown voltage and PDIV

| Parameter | Treated oil | Non-treated oil |
|--------------------------|-------------|-----------------|
| Breakdown | | |
| α | 37.5 kV | 35.3 kV |
| β | 4.9 | 5.5 |
| Partial discharge | | |
| α | 35.3 kV | 19.6 kV |
| β | 6.6 | 6.8 |

One can understand that appearance of PD at a relatively low voltage for non-treated oil comes from the fact that impurities are more likely to pass in the gap than with treated oil. The PDIV in treated oil, the breakdown voltage in non-treated oil and the breakdown voltage in treated oil are all very similar. This can be understood by looking at the different aspects of the gap after a breakdown. Two distinct types of failures can be observed. The most commonly observed is the superficial breakdown where arcing seems to have occurred in the oil at the surface of the PCB. In this case, the sample can be used again and shows similar breakdown voltages, as seen in Table 4. The second type of breakdown seems to happen inside of the varnish coating of the PCB and is only observed for the highest breakdown voltages. In both cases, it is observed that the varnish covering the edge of the copper trace has been damaged. The breakdown of the thin varnish coat on the copper would

result in a breakdown in oil when impurities are present in the gap. In treated oil, it is less likely to have impurities, hence the slightly higher breakdown voltage. In certain cases, impurities would not pass in the gap during the test and the voltage could be increased until the point where the varnish would then break in the complete gap length as seen in Fig. 12. This kind of failure occurred for 3 out of 20 samples. It can be seen in Fig. 13 that in the case of breakdown of the varnish, the arc has carved the surface and the fiberglass present inside of the PCB is made apparent.

One must note that, in a rectifier such as discussed in this paper, most conductive traces are not exposed to pure AC voltage, and some even experience unipolar voltages. It is reported in [8] that breakdown voltages are different when the traces are exposed to bipolar or unipolar waveforms. Thus, similar tests with unipolar waveforms are still needed.

Tab. 4: Repeated superficial breakdowns of one sample in non-treated oil, in chronological order

| Breakdown number | 1 | 2 | 3 | 4 |
|------------------------|------|------|------|------|
| Breakdown voltage (kV) | 30.9 | 32.4 | 26.8 | 29.2 |



Fig. 12: Left) Superficial dielectric breakdown, Right) Varnish dielectric breakdown (3 mm gap)

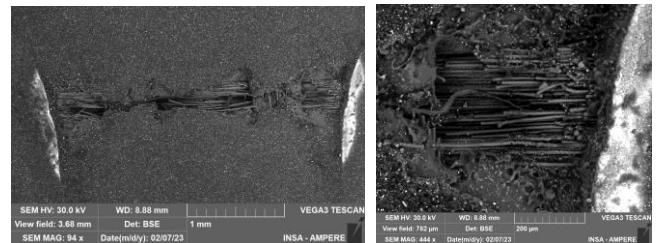


Fig. 13: Left) Electronic microscope capture of the trench created during the varnish breakdown event, Right) Zoom on the right electrode, with apparent fiberglass

4 Chemical compatibility of PCB-implemented rectifier components in oil

The immersion of power electronic components in oil is usually done in high power applications with press-pack components [11]. As seen in [6], the PCB implementation of a medium voltage low current rectifier uses traditionally packaged resistors and capacitors for the snubbers present on the rectifier board. The compatibility of these components with oil immersion is also investigated here.

4.1 Test set-up

The studied components are listed in the Table 5. A control sample is kept unaltered for each component. The test samples are initially dried at 80°C during 24 hours in order to remove any humidity that could be contained in the component. They are then weighted and photographed (Fig. 14). All of the components are immersed in the oil and stay in an oven at a given temperature for a week. After a week the components are removed from the oil and superficially wiped with blown nitrogen, and weighed. Control samples are also weighed again. The scale error is given as ± 5 mg. The procedure is then repeated, at a higher temperature. A mass decrease or increase of a component after immersion would indicate a disaggregation or an oil intake, respectively.

4.2 Experimental results

The results are shown in Fig. 15. The measured masses are normalized to the mass of the component after drying in order to remove offset between the test and control samples.

The most noticeable change is seen in the through-hole cemented resistor 1. A mass increase is measured in the test sample after the first immersion. The oil intake of the resistor can be observed in Fig. 16 where we see bulges appearing after the first immersion. Comparing with the capture of resistor 1 before immersion in Fig. 14, it can also be seen that the color of the cement changed to a darker tone after immersion. The fact that no further mass increase is observed after other immersions would mean that porosity in the cement structure filled up entirely during the first immersion. One should note that this interaction is not essentially problematic, as the resistance value was not measured to be outside of its rated tolerance after the mass increase. This observation only shows that there is an interaction with the oil.

Tab. 5: Tested components

| Component | Technology | Mass after drying |
|-------------|----------------------------------|-------------------|
| PCB | FR4 | 9.473 g |
| Diode | TO-247 | 6.043 g |
| Resistor 1 | Through-hole, cemented | 4.978 g |
| Resistor 2 | SMD, thin film | 225 mg |
| Capacitor 1 | Through-hole, polypropylene film | 1.345 g |
| Capacitor 2 | SMD, MLCC | 33 mg |



Fig. 14: Tested components before immersion, from top left to bottom right: PCB, diode, resistor 1, resistor 2, capacitor 1, capacitor 2.

The other components don't show significant change in their mass during the experiment. It can be seen that Capacitor 2 has the largest relative mass change. However, this is due to the fact that its initial mass of 33 mg is close to the scale error of ± 5 mg. The other component showing a separation between the test and control samples is the PCB. The mass change of less than 0.3% is not considered significant.

Capacitor 1 shows a visible change in the aspect of its insulating material as can be seen in Fig. 17. However, this is believed to be caused not by oil interaction but by temperatures exceeding the capacitor rated temperature of 80°C. Indeed, the color of the insulating material starts to change at the 100°C step.

The SMD components' masses are not affected by the oil immersion and they show no alteration during the whole experiment. This kind of component

is thus considered the preferred option for the implementation of the rectifier snubbers on the oil-immersed PCB, as they show no interaction with the oil.

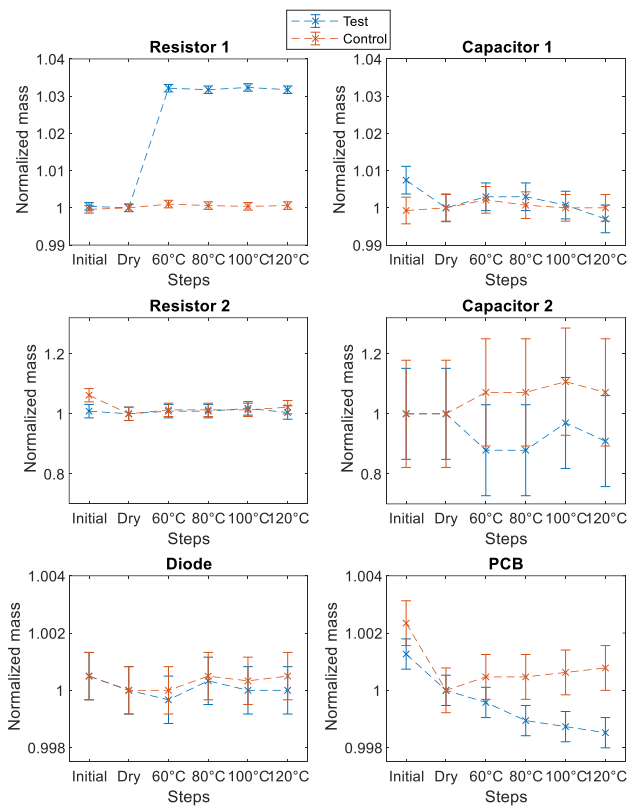


Fig. 15: Normalized mass of test and control samples with ± 5 mg error bars.

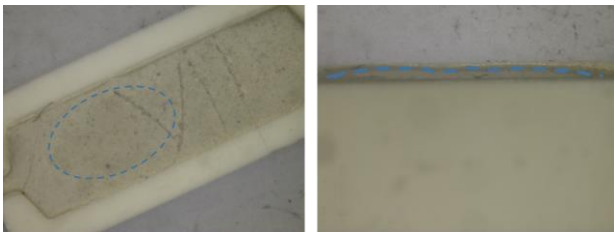


Fig. 16: Bulges appearing on the cement after the first immersion (VII is the component designator)



Fig. 17: Capacitor 1 insulating material after steps at temperature, from left to right, 80°C, 100°C and 120 °C.

5 Conclusion

The concept of integrating all of the medium voltage components of an MVDC SST in oil requires design guidelines for this environment. In particular, a PCB-implemented diode rectifier was studied in this paper regarding cooling, dielectric design and chemical compatibility. Patterned copper patches were shown to be usable as “flat heatsinks” increasing the exchange surface with oil while keeping a thin and flat form factor. The influence of the quality of the oil on the PDIV and breakdown levels was shown. Finally, it was shown that SMD components are suitable for oil immersion as they showed no degradations when exposed with prolonged immersion, even at high temperatures.

Acknowledgments

This work was supported by a grant overseen by the French National Research Agency as part of the “Investissements d’Avenir” Program (ANR-17-09-0001-01).

6 References

- [1] H. A. B. Siddique, S. M. Ali, and R. W. De Doncker, ‘DC collector grid configurations for large photovoltaic parks’, in *2013 15th European Conference on Power Electronics and Applications (EPE)*, Sep. 2013, pp. 1–10. doi: 10.1109/EPE.2013.6631799.
- [2] Sungrow, ‘SG250HX Multi-MPPT String Inverter for 1500 Vdc System’, SG250HX Datasheet, 2019.
- [3] P. Dworakowski, P. Le Métayer, C. Buttay, and D. Dujic, ‘Unidirectional step-up isolated DC-DC converter for MVDC electrical networks’, presented at the CIGRE Session 2022, Aug. 2022.
- [4] MIDEL, ‘MIDEL 7131 Product-Brochure’. Accessed: Sep. 30, 2022. [Online]. Available: <https://www.midel.com/app/uploads/2018/05/MIDEL-7131-Product-Brochure.pdf>
- [5] Y. He and D. J. Perreault, ‘Diode Evaluation and Series Diode Balancing for High-Voltage High-Frequency Power Converters’, *IEEE Transactions on Power Electronics*, vol. 35, no. 6, pp. 6301–6314, Jun. 2020, doi: 10.1109/TPEL.2019.2947578.
- [6] P. Le Metayer, C. Buttay, D. Dujic, and P. Dworakowski, ‘Medium Voltage Diode Rectifier Design for High Step-Up DC-DC Converter’, in *2022 24th European Conference on*

- Power Electronics and Applications (EPE'22 ECCE Europe)*, Hannover, Germany, Sep. 2022, pp. 1-9.
- [7] I. Wahyu Kuncoro, N. Pambudi, M. Biddinika, I. Widiastuti, M. Hijriawan, and M. K. Wibowo, 'Immersion cooling as the next technology for data center cooling: A review', in *Journal of Physics: Conference Series*, Dec. 2019, vol. 1402. doi: 10.1088/1742-6596/1402/4/044057.
- [8] A. Abdelmalik, M. Borge, A. Nysveen, L. E. Lundgaard, and D. Linhjell, 'Statistical analysis of dielectric breakdown of liquid insulated printed circuit boards', *IEEE Transactions on Dielectrics and Electrical Insulation*, vol. 23, pp. 2303–2310, Aug. 2016, doi: 10.1109/TDEI.2016.7556507.
- [9] S. Ramdas, P. Rajmane, T. Chauhan, A. Misrak, and D. Agonafer, *Impact of Immersion Cooling on Thermo-Mechanical Properties of PCB's and Reliability of Electronic Packages*. 2019. doi: 10.1115/IPACK2019-6568.
- [10] A. Fouineau, M. Guillet, B. Lefebvre, M.-A. Raulet, and F. Sixdenier, 'A Medium Frequency Transformer Design Tool with Methodologies Adapted to Various Structures', in *2020 Fifteenth International Conference on Ecological Vehicles and Renewable Energies (EVER)*, Sep. 2020, pp. 1–14. doi: 10.1109/EVER48776.2020.9243104.
- [11] I. A. Pires, R. Á. Silva, A. V. Rocha, M. P. Porto, T. A. C. Maia, and B. de J. C. Filho, 'Oil Immersed Power Electronics and Reliability Enhancement', *IEEE Transactions on Industry Applications*, vol. 55, no. 4, pp. 4407–4416, Jul. 2019, doi: 10.1109/TIA.2019.2915276.